HHS Public Access

Author manuscript

Nat Chem Biol. Author manuscript; available in PMC 2016 August 22.

Published in final edited form as:

Nat Chem Biol. 2016 April ; 12(4): 268–274. doi:10.1038/nchembio.2025.

Chemoproteomic profiling of host and pathogen enzymes active in cholera

Stavroula K. Hatzios[1,2,3], **Sören Abel**[#1,2,4], **Julianne Martell**[#5], **Troy Hubbard**[1,2,3], **Jumpei Sasabe**[1,2,3], **Diana Munera**[1,2,3], **Lars Clark**[1,2,3], **Daniel A. Bachovchin**[6], **Firdausi Qadri**[7], **Edward T. Ryan**[8,9], **Brigid M. Davis**[1,2,3], **Eranthie Weerapana**[5,*], and **Matthew K. Waldor**[1,2,3,*]

[1]Division of Infectious Diseases, Brigham and Women's Hospital, Boston, MA, USA

[2]Department of Microbiology and Immunobiology, Harvard Medical School, Boston, MA, USA

[3]Howard Hughes Medical Institute, Boston, MA, USA

[4]Department of Pharmacy, University of Tromsø (UiT), The Arctic University of Norway, Tromsø, Norway

[5]Department of Chemistry, Boston College, Chestnut Hill, MA, USA

[6]The Eli and Edythe L. Broad Institute, Cambridge, MA, USA

[7]International Centre for Diarrhoeal Disease Research, Bangladesh (ICDDR,B), Dhaka, Bangladesh

[8]Division of Infectious Diseases, Massachusetts General Hospital, Boston, MA, USA

[9]Department of Medicine, Harvard Medical School, Boston, MA, USA

[#] These authors contributed equally to this work.

Abstract

Activity-based protein profiling (ABPP) is a chemoproteomic tool for detecting active enzymes in complex biological systems. We used ABPP to identify secreted bacterial and host serine hydrolases that are active in animals infected with the cholera pathogen *Vibrio cholerae*. Four *V. cholerae* proteases were consistently active in infected rabbits, and one, VC0157 (renamed IvaP), was also active in human cholera stool. Inactivation of IvaP influenced the activity of other

[*]Correspondence should be addressed to M.K.W., (; Email: mwaldor@research.bwh.harvard.edu) or E.W. (; Email: eranthie.weerapana@bc.edu)

Author Contributions

S.K.H., E.W., and M.K.W. conceived the project and designed the experiments. S.K.H. generated the *V. cholerae* mutant strains, performed all biochemistry and ABPP experiments, and analyzed the MS data. S.A., T.H., and D.M. performed the rabbit infections. J.M. performed the MS experiments and assisted with MS data analysis. J.S. provided technical guidance on intelectin assays. L.C. assisted with the construction of *V. cholerae* mutant strains. D.A.B. synthesized FP-biotin. F.Q. and E.T.R. provided the human cholera stool used in this study. S.K.H., B.M.D., and M.K.W. wrote the manuscript.

Accession Codes

PRIDE Archive proteomics data repository. Data are available via ProteomeXchange with identifier PXD003000.

Competing Financial Interests Statement

The authors declare no competing financial interests.

secreted *V. cholerae* and rabbit enzymes in vivo, while genetic disruption of all four proteases increased the abundance and binding of an intestinal lectin—intelectin—to *V. cholerae* in infected rabbits. Intelectin also bound to other enteric bacterial pathogens, suggesting it may constitute a previously unrecognized mechanism of bacterial surveillance in the intestine that is inhibited by pathogen-secreted proteases. Our work demonstrates the power of activity-based proteomics to reveal host-pathogen enzymatic dialogue in an animal model of infection.

Introduction

During the course of infection, bacteria engage in a complex enzymatic dialogue with host cells: both pathogen and host express, and often secrete, enzymes that actively shape the biochemical landscape of a disease. Enzymes that are active at the host-pathogen interface can be critical for bacterial virulence or the host's response to infection and constitute potential therapeutic targets[1-3]. However, because post-translational regulation of protein function (e.g., through proteolytic activation, protein-protein, or protein-small-molecule interactions) can lead to an imperfect correlation between enzyme abundance and activity, traditional tools for analyzing disease-related changes in gene expression, such as transcriptional profiling and proteomics, may fail to reveal the active subset of enzymes in an infection.

Activity-based protein profiling (ABPP) is a chemoproteomic technique that enables the direct evaluation of enzyme activity within complex biological systems (Fig. 1a)[4]. Activity-based probes (ABPs) that are chemically tuned to react with the active site of a specific enzyme class facilitate selective detection, enrichment, and mass spectrometry (MS)-based identification of labeled proteins. Because these probes only react with functional enzymes, ABPP can distinguish between enzymes that are active and those that are expressed, but inactive. In recent years, ABPP has been applied to studies of microbial pathogenesis, primarily in tissue culture-based models of infection, enabling the characterization of several virulence-associated enzymes and host immune responses[5].

Vibrio cholerae, the Gram-negative bacterium that causes the severe and potentially fatal diarrheal disease cholera, is an extracellular pathogen that proliferates in the small intestine of infected hosts[6]. In vitro, *V. cholerae* has been shown to export numerous enzymes that may help shape its intestinal niche[7]; however, knowledge of the in vivo activity of these enzymes, and their interactions with host factors during infection, is extremely limited. Furthermore, the legions of host-secreted enzymes active in cholera remain ill defined.

To identify host and pathogen enzymes active during *V. cholerae* infection, we used ABPP to globally profile secreted serine hydrolase activity in the cecal fluid of *V. cholerae*-infected infant rabbits and human cholera stool (Fig. 1a). Serine hydrolases, which include proteases, esterases, lipases, peptidases, and amidases, comprise one of the largest enzyme families in nature[8] and can be selectively targeted by well-characterized fluorophosphonate (FP)-containing ABPs[9, 10] (Fig. 1b). We focused on serine hydrolases because they widely influence microbial pathogenicity[3, 11, 12], are often activated at the post-translational level[13] (and thus ideally studied by activity-based approaches), and are common drug targets[14-16].

We identified four secreted *V. cholerae* serine proteases that were consistently active in infected rabbits. One of these proteases, VC0157, renamed here IvaP (for **i**n **v**ivo-**a**ctivated **p**rotease), was also active in human cholera stool and was necessary for the extracellular activation of other *V. cholerae* enzymes in vivo. Catalytic inactivation of IvaP enhanced the activity of several host-secreted enzymes, while genetic disruption of all four *V. cholerae* proteases increased the abundance of intelectin, an intestinally secreted, D-galactofuranosyl-binding protein[17] that was found to bind *V. cholerae* cells in infected rabbits. Intelectin was also detected in human cholera stool and bound to other enteric pathogens in vitro, suggesting it may facilitate bacterial surveillance in the intestine. Taken together, these findings point to a potentially broad mechanism of pathogen recognition that is inhibited by secreted *V. cholerae* enzymes. Furthermore, our work demonstrates the power of activity-based proteomics to define host-pathogen enzymatic dialogue in an animal model of infection.

Results

ABPP identifies serine hydrolases active in cholera

We used ABPP to globally profile secreted serine hydrolases active in the cecal fluid of *V. cholerae*-infected rabbits and in human cholera stool. Orogastric inoculation of suckling rabbits with *V. cholerae* leads to a disease that closely resembles human cholera[18], and infected rabbits routinely accumulate 0.5–1 mL of cecal fluid (Fig. 1a). This fluid, which has a chemical composition similar to choleric stool[18], contains pathogen- and host-secreted products, in addition to ~10^9 colony-forming units (CFUs) per mL *V. cholerae*. We initially reacted cell-free supernatants from this fluid and human cholera stool with a fluorescently labeled ABP for serine hydrolases (FP-TAMRA)[10] (Fig. 1b), and SDS-PAGE analysis of reaction products revealed the presence of serine hydrolase activity (Fig. 1c). Subsequently, cecal fluid and stool isolates were reacted with FP-biotin (Fig. 1b), enabling affinity purification of active serine hydrolases[9, 19]. Proteins were purified in parallel from sample supernatants incubated with either FP-biotin or dimethyl sulfoxide (DMSO) (to account for non-specific protein enrichment) and analyzed by the MS method ABPP-multidimensional protein identification technology (ABPP-MudPIT)[20] in order to identify proteins whose recovery was ABP-dependent.

In total, 233 and 71 proteins exhibited activity-based enrichment from the cecal fluid of *V. cholerae*-infected rabbits and human cholera stool, respectively (Supplementary Results, Supplementary Fig. 1; Supplementary Tables 4–6; Supplementary Data Sets 1A and 2A). Host proteins were predominant in both sample sets (94% and 99% of the total enriched proteins from cecal fluid and stool, respectively), and the majority of stool-extracted proteins were enzymes with defined serine hydrolase activity, many involved in digestive processes (e.g., chymotrypsin-like elastases, trypsins, and pancreatic triacylglycerol lipase). Of the rabbit proteins identified, only a few have functional annotations in the UniProt database[21], including the digestive enzyme aminopeptidase N and the bacterial lipopolysaccharide-inactivating enzyme acyloxyacyl hydrolase; in addition, our data suggest that certain proteins may have redundant assignments within the database (e.g., UniProt accession numbers P12337 and G1SRL5, Supplementary Data Set 1A). However, of the 25 most

abundant proteins, ~75% contain predicted serine hydrolase domains (Supplementary Data Set 1A). Considerable overlap was observed between the active enzymes identified in human stool and cecal fluid (~45% of human enzymes had rabbit homologues; Supplementary Data Set 2A).

In contrast to the relatively large number of host enzymes, we detected only 14 affinity-purified proteins from *V. cholerae* in cecal fluid and one in human cholera stool; of these, 10 contain predicted serine hydrolase domains (Supplementary Tables 4 and 6; Supplementary Data Sets 1A and 2A). Four of these enzymes (VC0157, VC1200, VCA0812, and VCA0803) were detected in nearly all of the cecal fluid samples we tested (Supplementary Data Set 1C). Additional ABPP analyses indicated that all four of these enzymes were also active in the cell-free supernatants of *V. cholerae* biofilms, surface-associated communities of bacteria that have been shown to enhance *V. cholerae* infectivity and are believed to facilitate bacterial survival in aquatic reservoirs[22, 23] (Supplementary Data Set 3). VC0157 was the most abundant *V. cholerae* protein identified by ABPP in infected rabbits and biofilms (Supplementary Data Sets 1A and 3), and strikingly, was the only active *V. cholerae* enzyme detected in human cholera stool (Supplementary Data Set 2A).

Bioinformatic analyses revealed that VC0157, VC1200, VCA0812, and VCA0803 are putative secreted serine proteases[24] with conserved C-terminal domains found in other bacterial peptidases[25, 26] (Fig. 2). VCA0803 and VC1200, also known as VesA and VesB, respectively, have trypsin-like activity[26, 27]; similarly, VCA0812 contains a trypsin-like peptidase domain[24], though its activity has not been validated biochemically. VesA and VesB, along with VCA0812, are putative substrates of the type II secretion system of *V. cholerae*, which is also responsible for the export of cholera toxin, a critical virulence factor of *V. cholerae* that is cleaved by VesA and VesB in broth culture supernatants[27]. In contrast, relatively little is known about VC0157, a putative alkaline serine protease which we have renamed IvaP. IvaP contains a subtilisin-like S8 peptidase domain, which is typically associated with broad substrate specificity[28], and has been previously detected in proteomic analyses of outer membrane vesicles[29]. In addition, genetic deletion of the *ivaP* gene has been shown to reduce degradation of the biofilm matrix protein RbmA in certain *V. cholerae* mutant backgrounds[30]. IvaP contains several predicted protein domains that are typically sites of post-translational processing, including an N-terminal signal sequence, a putative peptidase inhibitor I9 domain, and a C-terminal bacterial pre-peptidase (PPC) domain (Fig. 2); cleavage of the I9 and/or PPC domains found in IvaP has been associated with the activation of related proteases[31, 32].

IvaP undergoes significant extracellular processing

We investigated the expression, proteolytic processing, and activity of IvaP in cell-free supernatants from exponential phase, stationary phase, and biofilm cultures of *V. cholerae*. Through parallel in-gel fluorescence and immunoblotting analyses of FPTAMRA-labeled supernatants from wild-type and Δ*ivaP V. cholerae* (Fig. 3a), we discovered that IvaP is absent from exponential phase culture supernatants, but is present as two distinct protein species in the secreted fraction of stationary phase cultures. Comparative analyses of supernatants from stationary phase cultures and biofilms grown for 24 or 48 h suggest that

precursor proteins (~45–49 kDa) are successively cleaved to generate the fully processed (~40 kDa) enzyme, whose identity was confirmed by MS (Supplementary Fig. 2). Only tryptic peptides corresponding to a truncated enzyme of similar molecular weight (~40 kDa), which lacks the signal peptide and I9 peptidase inhibitor domain, were detected in our ABPP-MudPIT analyses of biofilm supernatants and cecal fluid (Supplementary Fig. 3). However, the higher molecular weight IvaP precursors we detected in our gel-based ABPP analyses of stationary phase culture supernatants also exhibited serine hydrolase activity (Fig. 3a). Thus, IvaP can be processed into several active forms, and the extent of IvaP processing varies under different growth conditions.

IvaP was not detected in cell lysates of either exponential or stationary phase cultures by immunoblotting (Supplementary Fig. 4), nor were any of its peptides detected in activity-based proteomic analyses of these samples (Supplementary Data Set 4), suggesting that IvaP produced by stationary phase cells is rapidly released into culture supernatants. Interestingly, previous RNA-seq analyses indicate that *ivaP* transcript abundance in exponential phase cultures does not differ significantly from transcript abundance in vivo (i.e., in cecal fluid)[33], despite the marked difference in secreted IvaP between these samples. These data suggest that distinct post-transcriptional regulatory processes may govern IvaP in vitro and in vivo, in addition to the post-translational cleavage events discussed above, and underscores the distinction of ABPP, which detects protein activity, from RNA or other proteomic analyses, which do not.

We mutated the predicted catalytic serine of IvaP (Ser361) to an alanine to test whether autoproteolysis mediates IvaP processing. Western blot analyses revealed that IvaP^{S361A} from the mutant strain (Δ*ivaP::ivaP*^{Ser361Ala}) has a higher molecular weight (~49 kDa) than IvaP from the wild-type strain in biofilm supernatants (Fig. 3b). Additionally, supernatants from the mutant strain lacked apparent IvaP activity when assayed with FP-TAMRA. Together, these data indicate that Ser361 is required for IvaP activity and that autoproteolysis contributes to IvaP's post-translational processing. Finally, while our data suggest that the most serine hydrolase activity in biofilm supernatants stems from IvaP (Fig. 3a; Supplementary Data Set 3), its activity does not appear to be linked to biofilm formation (Supplementary Fig. 5).

IvaP influences the activity of other serine hydrolases

Because proteolysis is a common mechanism of enzyme activation and inhibition, we hypothesized that IvaP might alter the activity of other secreted pathogen and/or host enzymes via proteolytic cleavage. Interestingly, both VesA and VesB, two of the four secreted *V. cholerae* proteases that were active in biofilms and cecal fluid, contain propeptides that may regulate their activation[26].

To determine whether IvaP might influence the activity of other enzymes during infection, we compared the activity of serine hydrolases in the cecal fluid of rabbits infected with either wild-type *V. cholerae* or *V. cholerae* expressing the catalytically inactive IvaP^{S361A} (Δ*ivaP::ivaP*^{Ser361Ala}). We identified four *V. cholerae* serine hydrolases, in addition to IvaP, whose activity was higher (>5-fold change in spectral counts with $P \leq 0.05$) in the cecal fluid of rabbits infected with wild-type versus mutant *V. cholerae* (Fig. 4a; Supplementary Table

7; Supplementary Data Set 1B): the previously described VCA0812 and VesB; the thermolabile hemolysin VCA0218, which exhibits phospholipase activity in vitro[34]; and the surface-exposed, outer membrane-associated phospholipase VolA (VCA0863), which has been shown to hydrolyze lysophosphatidylcholine (LPC) in vitro and may facilitate bacterial uptake of host-derived fatty acids in vivo[35]. Additionally, we identified 2 rabbit serine hydrolases that were less active in animals infected with wild-type *V. cholerae* (>5-fold reduction in spectral counts with $P \leq 0.05$): kallikrein 1 (KLK1), a trypsin-like peptidase that regulates vascular tone[36], and cholesterin esterase (aka bile-salt activated lipase), a digestive enzyme that hydrolyzes triglycerides and other lipid esters in the intestine[37] (Fig. 4a; Supplementary Table 8; Supplementary Data Set 1B). Collectively, these findings suggest IvaP influences the activity of other pathogen-secreted and host serine hydrolases that may shape the intestinal niche of *V. cholerae*.

To further investigate the altered activity of host and bacterial lipases associated with inactive IvaP and the proteases it appears to regulate, we performed comparative lipidomic analyses of the total (esterified and non-esterified) and free (non-esterified) fatty acids in cecal fluid from rabbits infected with wild-type *V. cholerae* or *V. cholerae* lacking the genes for all 4 secreted proteases found to be active in vivo (*ivaP*, *vesA, vesB*, and *vca0812; Δ*quad). We used Δquad *V. cholerae* for these and subsequent analyses in order to maximize potential protease-dependent phenotypes. Our lipidomic analyses revealed that the average amount of total C16:0 lipids (i.e., palmitic acid and palmitate esters) was ~5-fold greater in wild-type-infected animals (Fig. 4b; Supplementary Data Set 5). In contrast, we did not observe a significant difference in the average free palmitic acid content of these samples, suggesting that the abundance of palmitate esters may be selectively affected by the *V. cholerae* proteases. No significant differences were detected in the average levels of the remaining 32 fatty acids we analyzed (Supplementary Data Set 5).

V. cholerae proteases alter host protein abundance

To identify additional secreted and cell-associated bacterial and host proteins present in the context of an infection, we conducted proteomic analyses of cecal contents (unfractionated cecal fluid) from rabbits infected with wild-type *V. cholerae* and from unfractionated human cholera stool. In the cecal contents of wild-type-infected rabbits, we detected 1330 proteins (405 *V. cholerae*, 925 rabbit) with ≥2 spectral counts (Supplementary Data Set 6). The *V. cholerae* proteins included key contributors to virulence (e.g., both subunits of cholera toxin and TcpA, the major subunit of a pilus that is *V. cholerae*'s principal intestinal colonization factor[6]). Notably, we did not detect IvaP or the other 3 *V. cholerae* proteases identified by ABPP-MudPIT in these analyses, which underscores the ability of ABPP to enhance detection of low-abundance enzymes. Host proteins included several rabbit immunoglobulins and hemoglobin subunits; however, the majority of rabbit proteins we detected in cecal fluid are uncharacterized. We identified fewer total proteins in a parallel whole-proteome analysis of human cholera stool (29 *V. cholerae*, 464 human) (Supplementary Data Set 7), perhaps because the human sample was more dilute than cecal fluid. However, 27 of the stool-derived bacterial proteins we detected were also present in cecal fluid. A number of immunoglobulins were also detected in human cholera stool, as well as several digestive proteases (e.g., chymotrypsin-like elastases).

Comparative whole-proteome analyses of cecal fluid from rabbits infected with wild-type *V. cholerae* or the Δquad mutant revealed 9 host proteins that were significantly more abundant (>5-fold change in spectral counts with a lower confidence limit >1) in Δquad-infected animals, suggesting that they may be degraded by one or more of the deleted enzymes; we did not detect any bacterial proteins that were significantly enriched in these mutant samples (Fig. 4c; Supplementary Table 9; Supplementary Data Set 6). The host proteins we identified included a putative cathepsin (cysteine-type) protease, the phospholipid-binding protein annexin A1, a putative chymotrypsin-like elastase (serine-type protease), and a galactoside-binding galectin. In addition, our proteomic analyses identified an uncharacterized rabbit protein (UniProt accession number G1U048) with 88% amino acid sequence identity (Supplementary Fig. 6) to human intelectin, an intestinally secreted, D-galactofuranosyl-binding protein[17]. Because galactofuranose is found in a variety of microbial, but not mammalian, glycoconjugates[38], intelectin has been proposed to facilitate mucosal adhesion and/or phagocytic uptake of bacterial pathogens in the host and may therefore be a rational target for secreted bacterial proteases. Thus, although protease deletion (of IvaP alone, or of all four proteases) did not significantly alter *V. cholerae* intestinal colonization (Supplementary Fig. 7 and 8) or cecal fluid accumulation in infected rabbits, our proteomic and lipidomic data suggest that secreted *V. cholerae* serine proteases regulate host factors that may modulate pathogen metabolism and interactions with the infected host.

Intelectin binds V. cholerae and other enteric bacteria

Human intelectin consists of two isoforms (intelectin-1 and intelectin-2) with 91% amino acid sequence identity[39]. Previous studies have demonstrated that intelectin-1 is constitutively expressed at high levels in the murine small intestine, whereas expression of intelectin-2 is strongly induced by intestinal nematodes, suggesting that intelectin plays a role in the intestinal innate immune response[40, 41]. Both secreted and membrane-associated forms of intelectin localize along the brush border of enterocytes[39], which is the site of *V. cholerae* colonization[18]. Furthermore, intelectin-1 was identified in duodenal biopsies from cholera patients[42], and we detected both isoforms of the protein in human cholera stool (Supplementary Data Set 7B). Human intelectin-1 has been shown previously to bind *Mycobacterium bovis* bacillus Calmette-Guérin (BCG) in a Ca^{2+}-dependent manner in vitro[43]; however, intelectin binding to *V. cholerae* or other enteric bacteria has not been demonstrated.

We developed an in vitro assay using purified human intelectin-1 to assess whether *V. cholerae* or other enteric pathogens are bound by this protein. Unbound, wash (with Ca^{2+}-containing buffer), and elution (with EDTA) fractions were analyzed by SDS-PAGE and immunoblotting with a polyclonal intelectin-1 antibody. A major band corresponding to the molecular weight of purified intelectin (likely in trimeric form, as previously observed[43]) was detected in the unbound and elution fractions of intelectin-treated *V. cholerae* cells, but not mock-treated cells (Fig. 5a), demonstrating that intelectin binds *V. cholerae* in a Ca^{2+}-dependent manner. Intelectin bound similarly to all additional bacterial species that we assayed, including Gram-negative (Escherichia coli, Vibrio parahaemolyticus, Salmonella enterica) and Gram-positive (*Listeria monocytogenes*, *Staphylococcus aureus*) species (Fig. 5b; Supplementary Fig. 9). The cell-surface diversity of these bacterial species suggests that

intelectin may bind to multiple components of the bacterial cell envelope (e.g., capsular or outer-membrane glycoproteins/glycolipids or cell-wall glycans).

V. cholerae proteases decrease intelectin binding in vivo

Immunoblotting analyses of proteins associated with *V. cholerae* cells that were isolated from the ceca of infected rabbits suggest that intelectin also binds to *V. cholerae* during infection. As observed in our in vitro assays with purified intelectin, the EDTA-eluted protein fraction contained an ~120-kDa species that was recognized by polyclonal intelectin-1 antisera (Fig. 5c). This species was far less abundant in the Ca^{2+}-wash fraction and was not detected in cell-free supernatants of cecal contents, suggesting that most intelectin in the ceca of *V. cholerae*-infected rabbits is cell-associated. Addition of the reducing agent dithiothreitol to the EDTA-eluted fraction converted the ~120-kDa band to a single band of ~38 kDa, consistent with the molecular weight of glycosylated human intelectin monomers[43], which provides further support for the idea that the ~120-kDa species is a disulfide-linked intelectin trimer.

Analyses of bacteria-associated intelectin were also performed with Δquad *V. cholerae* isolated from infected rabbits. As observed in our proteomic analyses, which detected increased intelectin in the cecal contents of rabbits infected with Δquad versus wild-type *V. cholerae*, there was a consistent and substantial (~4–9-fold) increase in the amount of intelectin eluted from Δquad *V. cholerae* compared to wild-type bacterial cells (Fig. 5c; Fig. 5d). Notably, wild-type and Δquad *V. cholerae* grown in vitro exhibited approximately equal intelectin binding (Supplementary Fig. 10), suggesting these strains have similar cell surfaces. Collectively, these observations suggest less intelectin degradation occurs in the absence of the secreted *V. cholerae* serine proteases, which may, in turn, enable increased intelectin binding to *V. cholerae* cells.

We monitored the proteolysis of recombinant human intelectin-1 in the presence of cell-free cecal fluid supernatants from rabbits infected with wild-type or Δquad *V. cholerae* to determine if intelectin degradation is enhanced by the *V. cholerae* proteases. Immunoblotting revealed that intelectin was degraded more rapidly by cecal fluid containing the *V. cholerae* proteases (Fig. 5e); however, incubation with either extract induced a nominal decrease in the molecular weight of the protein, and cecal fluid lacking the *V. cholerae* proteases was still capable of degrading intelectin, albeit more slowly. Taken together, these data suggest that the *V. cholerae* proteases accelerate intelectin degradation in vitro.

Discussion

We used activity-based chemoproteomic analyses to characterize *V. cholerae* and host intestinal serine hydrolases that are active during infection and identified four pathogen-secreted serine proteases that were consistently active in infected rabbits. One of these enzymes, IvaP, the product of a previously uncharacterized locus (*vc0157*), was also active in human cholera stool and influenced the activities of other bacterial and host serine hydrolases during infection. The apparent requirement of IvaP for the activity of other pathogen-secreted serine proteases (Fig. 4a) suggests this enzyme may be at the helm of an extracellular proteolytic cascade in vivo. Intracellular IvaP was not detected by

immunoblotting or ABPP (Supplementary Fig. 4; Supplementary Data Set 4), suggesting that IvaP-dependent activation of other enzymes (e.g., VesB, VCA0812, VolA) occurs extracellularly. IvaP may regulate these enzymes through direct proteolytic cleavage (e.g., of a prodomain) or through indirect mechanisms (e.g., by cleaving an upstream activator or inhibitor). While similar trans-activating *Vibrio* proteases have been described previously in vitro[44], our data suggest that IvaP spearheads mechanisms of proteolytic activation that are functional during infection.

In addition, IvaP appears to negatively regulate the activity of two host enzymes, KLK1 and cholesterin esterase, in infected rabbits (Fig. 4a). KLK1 belongs to the tissue kallikrein family, a group of 15 secreted serine proteases with a broad range of physiological functions[36]. KLK1 cleaves low-molecular-weight kininogen, a precursor of the vasodilator bradykinin[36]. Notably, infant rabbits infected with *V. cholerae* exhibit severe capillary congestion in intestinal tissues compared to mock-infected animals[18], and it is possible that IvaP may play a role in controlling intestinal capillary tone during *V. cholerae* infection by directly or indirectly inhibiting KLK1 activity.

Cholesterin esterase hydrolyzes a wide range of triglycerides and other lipid esters that may be substrates for pathogen lipases during infection[37]. Interestingly, our data indicate that the VolA lipase of *V. cholerae*, which has been shown to hydrolyze the intestinal lipid ester LPC in vitro[35], is active in infected rabbits, and that IvaP increases VolA activity in vivo (Fig. 4a). Furthermore, palmitate (C16:0) esters, which are common building blocks of triglycerides and LPC[45, 46], are more abundant during infection with wild-type than Δquad *V. cholerae* (Fig. 4b). These findings suggest that IvaP, and/or one of the other two pathogen-secreted proteases it regulates in vivo, may alter the lipid content of cecal fluid by inhibiting host lipase activity, which may ultimately increase the availability of intestinal lipids for bacterial consumption.

Our data also point to a role for these pathogen-secreted proteases in inhibiting intelectin binding to *V. cholerae* and add crucial in vivo evidence to the hypothesis that intelectin facilitates microbial recognition by the host. We show for the first time that intelectin binds to the surface of a bacterial pathogen during infection (Fig. 5c), and that this lectin binds to diverse enteric bacterial pathogens (Fig. 5b). Previous studies revealed that intelectin 1) recognizes non-mammalian sugars[17, 47], 2) enhances mycobacterial phagocytosis and adhesion to epithelial cells in vitro[43], and 3) has increased expression in response to nematode infection[40, 41]. Still, many questions remain regarding intelectin's potential role in the innate immune response to *V. cholerae*, and presumably to other enteric pathogens, as well. First, what are the consequences of intelectin binding to the pathogen surface? That is, does intelectin binding promote pathogen clearance, and do *V. cholerae*'s protease(s), which mediate lectin degradation, constitute a pathogen evasion strategy? Alternatively, it is possible that *V. cholerae* uses intelectin binding to its surface to promote bacterial adhesion to the intestinal epithelium. Second, does intelectin recruit other host proteins to bound bacteria? The recently solved crystal structure of trimeric human intelectin-1 indicates that saccharide binding occurs along one face of the trimer[47], raising the possibility that the distal end of the complex may interact with other host proteins. Third, do the alternative roles of intelectin as both an intestinal receptor for the iron-binding protein lactoferrin[48] and

an adipocytokine (aka omentin)[49] influence its interactions with, or impact on, microbial pathogens? Regardless of the answers to these questions, the widespread binding of intelectin to diverse bacteria suggests that this lectin could be considered a receptor for a microbe-associated molecular pattern.

Finally, our work demonstrates the power of activity-based proteomics to interrogate enzyme-mediated interactions between a pathogen and its host in an animal model of infection. By capturing enzymes active in *V. cholerae*-infected rabbits, we identified four pathogen-secreted proteases that alter the biochemical composition of cecal fluid, decrease the activity of host serine hydrolases, and inhibit bacterial binding by a host-secreted lectin. Our findings highlight the ability of ABPP to dissect complex enzymatic crosstalk at the host-pathogen interface and suggest that application of this approach to other animal models of microbial infection could yield important insights into the underlying enzymology of diverse infectious diseases.

Online Methods

Growth conditions and media

Bacteria were grown at 37 °C in LB (*V. cholerae*, *V. parahaemolyticus*, *E. coli*, *S. enterica*), Tryptic Soy (*S. aureus*), or Brain Heart Infusion (*L. monocytogenes*) broth or on agar plates supplemented as needed with 200 μg/mL (*V. cholerae*, *V. parahaemolyticus*, *L. monocytogenes*) or 500 μg/mL (*S. aureus*) streptomycin. Exponential (OD_{600}~0.4–0.8) and stationary (OD_{600}~2–3) phase cultures of *V. cholerae* were grown with shaking at 250 rpm from an overnight culture diluted 1:100 in fresh medium to the desired bacterial density. Biofilm cultures were grown in 6-well cell culture plates or borosilicate glass tubes without shaking for 24 or 48 h from an overnight culture diluted 1:1,000 in fresh medium.

Strains and plasmids

A complete list of the strains, plasmids, and primers used in this study can be found in the Supplementary Information (Tables 1–3).

V. cholerae mutant strains were generated from the *V. cholerae* El Tor clinical isolate C6706 using standard allelic exchange techniques as previously described[50] and derivatives of the suicide plasmid pCVD442. *E. coli* strains DH5α*λpir* and SM10*λpir* were used for cloning and conjugating DNA into *V. cholerae*, respectively. Cloned constructs were validated by DNA sequencing and transformed via electroporation. *V. cholerae* mutations were confirmed by PCR.

Strain Δ*ivaP* was generated by deleting nucleotides (nt) 121 through 1579 of the *ivaP* (*vc0157*) gene with plasmid pCVD442-Δ*ivaP*. Strain Δquad was generated via consecutive deletion of the *vesA* (*vca0803*, nt 25–866), *vesB* (*vc1200*, nt 31–1108), and *vca0812* (nt 31–1274) genes in strain Δ*ivaP* with plasmids pCVD442-Δ*vcA0803*, pCVD442-Δ*vc1200*, and pCVD442-Δ*vca0812*, respectively. Strain Δ*ivaP::ivaP*^{Ser361Ala} (S361A) was generated using plasmid pCVD442-*ivaP*^{Ser361Ala} and Δ*ivaP* as the recipient strain. Strain Δ*vpsA* was generated from a *V. cholerae* mutant that constitutively expresses GFPmut3 under the

control of the lac promoter (*V. cholerae* C6706 Δ*lacZ::Plac-gfp*) using plasmid pAJH9, a kind gift from Paula Watnick (Children's Hospital, Boston, MA, USA).

Plasmids pCVD442-Δ*ivaP*, pCVD442-Δ*vcA0803*, pCVD442-Δ*vc1200*, and pCVD442-Δ*vca0812* were constructed by PCR amplification of the DNA regions flanking gene *vc0157*, *vca0803*, *vc1200*, or *vca0812*, respectively (for primers, see Supplementary Table 3). These PCR products were spliced together via overlap extension PCR and ligated into pCVD442 as previously described[50]. Plasmid pCVD442-*ivaP*^{Ser361Ala} was constructed by PCR amplification of the *ivaP* gene with flanking regions, followed by ligation into pCVD442. The encoded Ser361 was mutated to an Ala by QuikChange mutagenesis (Agilent).

Rabbit infections and intestinal colonization studies

All animal protocols were reviewed and approved by the Harvard Medical Area Standing Committee on Animals. Experiments were performed essentially as previously described[51]. To prepare the infective inoculum, a mid-exponential culture of *V. cholerae* was harvested by centrifugation (5,000 × g, rt, 10 min), resuspended in sodium bicarbonate solution (2.5 g in 100 mL; pH 9) and adjusted to a concentration of 2×10^9 CFU/mL. Two- to three-dayold male and female New Zealand White infant rabbits (Pine Acre Rabbitry, Norton, MA, USA) were treated with Zantac (ranitidine hydrochloride; GlaxoSmithKline) by intraperitoneal injection (2 μg/g body weight) 3 h prior to infection. Animals were infected with 0.5 mL of the inoculum by gavage using a size 4 French catheter (Arrow International). Rabbits were housed with their mother and littermates for the duration of the experiment and euthanized by intracardial injection of 2.5 mL KCl (2 M, injection grade, USP; Hospira) after anesthesia with isoflurane (Butler Schein Animal Health) as soon as they developed severe diarrhea or by 20 h post-infection. When possible, infected animals of a single litter were used to reduce biological variability within a given experiment; thus, sample size was limited both by the number of rabbits per litter (typically 6) and the number of littermates that developed clinical signs of disease post-infection (e.g., accumulated sufficient cecal fluid for MS analyses). No randomization or blinding was performed; animals were equally distributed among experimental groups based on their weight and size.

At necropsy, the entire intestinal tract from the duodenum to the rectum was removed. The cecal fluid was collected with a syringe and 26 G needle (Becton, Dickinson, and Co.). Tissue samples (3-cm long) from the proximal, middle, and distal small intestine and colon were collected. Tissue samples were homogenized in 1 mL sterile phosphate-buffered saline (PBS) using a Mini-Beadbeater-16 and 3.2-mm stainless steel beads (BioSpec). CFUs of *V. cholerae* were enumerated by plating serial dilutions of tissue homogenates and cecal fluid on LB agar plates supplemented with 200 μg/mL streptomycin.

Human stool collection

Rice water stool was collected from a patient with culture-confirmed *V. cholerae* O1 cholera at the International Centre for Diarrhoeal Disease Research in Dhaka, Bangladesh (ICDDR,B) and immediately snap frozen and stored at −80 °C until analysis. This work was

approved by the Ethical Review and Research Review Committee of the ICDDR,B and the Institutional Review Board of Massachusetts General Hospital.

Preparation of proteomes for gel-based ABPP, ABPP-MudPIT, and proteomic analyses

Cecal fluid (~0.1–1 mL per rabbit) was stored on ice immediately following extraction. For gel-based ABPP and ABPP-MudPIT analyses, the fluid was centrifuged (20,817 × g, 4 °C, 5 min), and the resulting supernatant was syringe-filtered through a 0.45-μm, 13-mm PVDF filter (EMD Millipore). For ABPP-MudPIT analyses of cecal fluid from wild-type *V. cholerae*-infected rabbits, multiple cecal fluid isolates were pooled prior to probe labeling. For comparative ABPP-MudPIT analyses of cecal fluid from wild-type and S361A *V. cholerae*-infected rabbits, individual cecal fluid isolates were labeled with probe. For proteomic analyses, unfractionated fluid was frozen at −80 °C prior to in-solution trypsin digestion. Human cholera stool was thawed on ice and centrifuged at low speed (500 × g, rt, 10 min) to separate debris from the proteome prior to in-solution trypsin digestion of the unfractionated fluid or isolating the cell-free supernatant for probe labeling as described above.

Exponential and stationary phase *V. cholerae* cultures for comparative gel-based ABPP analyses were normalized by OD_{600} and centrifuged (6,000 × g, 4 °C) for 10 or 20 min, respectively. Cultures for ABPP-MudPIT analyses were similarly processed, but without prior normalization. Harvested cells were washed twice with 1 mL PBS and frozen at −80 °C. Cells were thawed on ice and resuspended in 0.3 mL PBS, lysed by sonication (Fisher Scientific Model 60 Sonic Dismembrator), and centrifuged at 4 °C for 10 min at 20,817 × g, or for 1 h at 100,000 × g, to clarify cell lysates for gel-based ABPP or ABPP-MudPIT analysis, respectively. Supernatants from exponential cultures were filtered through 0.22-μm, 33-mm PVDF filters (EMD Millipore), and stationary culture supernatants were twice filtered through 0.45-μm and 0.22-μm filters. Biofilm cultures were centrifuged (5,000 × g, 4 °C, 10 min), and the culture supernatants were twice filtered as described above. Cell-free supernatants from exponential, stationary, and biofilm cultures were concentrated 20- to 100-fold using Amicon centrifugal filter units with an Ultracel-10 membrane (EMD Millipore). Protein concentrations were measured using the Pierce Coomassie Plus (Bradford) Assay Kit (Life Technologies).

Gel-based ABPP analyses

Cell-free supernatants from biofilm cultures (1 mg/mL), cecal fluid (0.6 mg/mL), and human cholera stool (0.3 mg/mL) and cell lysates from exponential and stationary phase *V. cholerae* cultures (1 mg/mL) were reacted with 2 μM FP-TAMRA (ActivX TAMRA-FP Serine Hydrolase Probe; Thermo Scientific) for 1 h at rt in a 50-μL volume. Reactions were quenched by adding 50 μL 2X SDS-PAGE loading buffer and heating the samples for 5 min at 95 °C. For comparative analyses of cell-free supernatants from exponential, stationary, and biofilm cultures of *V. cholerae*, samples were normalized to 0.25 mg/mL in Milli-Q water prior to reaction with 2 μM FPTAMRA. Samples were separated by SDS-PAGE alongside a fluorescently labeled protein standard using 10% NuPAGE Bis/Tris precast gels (Life Technologies). In-gel fluorescence was detected using a Typhoon 9400 Variable Mode Imager (GE Healthcare). Total protein was visualized using SimplyBlue SafeStain (Life

Technologies). All gel-based ABPP analyses were repeated at least twice with consistent results.

Western blot analyses

For comparative analyses of cell lysates or cell-free supernatants from exponential, stationary, or biofilm cultures of *V. cholerae*, protein samples were separated by SDS-PAGE alongside a pre-stained protein standard using 10% NuPAGE Bis/Tris precast gels (Life Technologies) and transferred to nitrocellulose using an iBlot gel transfer device (Life Technologies). Protein bands were detected by immunoblotting with a custom anti-IvaP antibody generated using the 15 amino acid peptide CLSDRSTKGKVSDTQ (1:1000 dilution, mouse polyclonal; GenScript) or an anti-RNA polymerase alpha antibody (1:100,000, mouse monoclonal; Santa Cruz Biotechnology, sc-101597) and a horseradish peroxidase-conjugated secondary antibody (1:2000 dilution, goat anti-mouse IgG-HRP; Santa Cruz Biotechnology, sc-2005) and chemiluminescent reagents (Life Technologies). For Western blot analyses of intelectin, samples were separated by SDS-PAGE using 4–12% NuPAGE Bis/Tris precast gels and processed as above using an anti-human intelectin-1 antibody (1:2000 dilution, sheep polyclonal; R&D Systems, AF4254) and a rabbit anti-sheep IgG-HRP secondary antibody (1:5000 dilution; Southern Biotech, 6150-05). All immunoblotting analyses were performed twice at minimum with consistent results.

Probe labeling and affinity purification of labeled proteins for ABPP-MudPIT

Cell-free supernatants from biofilm cultures (300 μL, 1 mg/mL), human cholera stool (650 μL, 0.25 mg/mL), and cell lysates from exponential and stationary phase *V. cholerae* cultures (500 μL, 1 mg/mL) were labeled with FP-biotin (5 μM; synthesized as previously described[19]; characterization matched literature values) or DMSO for 1 h at rt. Pooled cecal fluid isolates from wild-type *V. cholerae*-infected rabbits (Sample A: 245 μL, 0.5 mg/mL; Sample B: 1.9 mL, 0.3 mg/mL; Sample C: 210 μL, 0.4 mg/mL; Supplementary Fig. 1, Supplementary Tables 4 and 5, Supplementary Data Set 1A) and individual isolates for comparative analyses of wild-type and S361A *V. cholerae*-infected rabbits (450 μL, 0.3 mg/mL; Fig. 4a, Supplementary Tables 7 and 8, Supplementary Data Set 1B) were similarly labeled with probe. A NAP-5 column (GE Healthcare) was used to remove the unreacted probe from each sample. The resulting probe-labeled protein (eluted in 1 mL PBS) was added to a solution of SDS/PBS (1.2% (w/v) final SDS concentration), heated for 5 min at 90 °C, and then diluted to a final SDS concentration of 0.2% with PBS. The solutions were incubated with 100 μL streptavidin-agarose beads (Thermo Scientific) at 4 °C for 16 h, and then at rt for 3 h. The beads were washed with 0.2% SDS/PBS (5 mL), PBS (3 × 5 mL), and water (3 × 5 mL). The beads were pelleted by centrifugation (1400 × g, 4 °C, 3 min) between washes.

On-bead trypsin digestion

The washed beads were suspended in 6 M urea in PBS (500 μL) and dithiothreitol (10 mM final concentration, diluted from a 20X stock in water) and incubated at 65 °C for 15 min. Iodoacetamide (20 mM final concentration, diluted from a 20X stock in water) was then reacted with the samples at 37 °C for 30 min. Following reduction and alkylation, the beads were pelleted by centrifugation (1400 × g, 4 °C, 3 min) and suspended in 200 μL of 2 M

urea, 1 mM $CaCl_2$ (diluted from a 100X stock in water), and sequencing-grade modified trypsin (2 μg; Promega) in PBS. The digestion was allowed to proceed overnight at 37 °C. The digested peptides were separated from the beads using a Micro Bio-Spin column (BioRad). The beads were washed twice with 50 μL ultrapure water, and formic acid (15 μL) was added to the eluted peptides, which were stored at −20 °C until MS analysis.

In-solution trypsin digestion

Unfractionated cecal fluid and human cholera stool samples were vortexed with 1/10 volume of 100% (w/v) trichloroacetic acid in PBS and frozen overnight at −80 °C. Samples were thawed on ice, centrifuged (20,817 × g, 4 °C, 10 min), and washed 3 times with cold acetone (500 μL). Samples were sonicated and centrifuged (2655 × g, 4 °C, 10 min) between washes. Acetone-washed pellets were air-dried and resuspended by sonication in 100 μL PBS containing 2.4 M urea and 70 mM ammonium bicarbonate, treated with 15 mM dithiothreitol, and incubated at 65 °C for 15 min. Iodoacetamide (12.5 mM final concentration) was then reacted with the samples for 30 min at rt. PBS (120 μL) was added to each sample, and protein concentrations were measured using the Pierce Coomassie Plus (Bradford) Assay Kit (Life Technologies). Samples were adjusted to 0.5 mg/mL in PBS and divided into 2 technical replicates of equal volume (90 μL). Samples were incubated with sequencing-grade modified trypsin (2 μg; Promega) and 1 mM $CaCl_2$ and digested overnight at 37 °C. Digested peptides were treated with formic acid (5 μL) and centrifuged (100,000 × g, 4 °C, 1 h) to remove any remaining particulates. Supernatants were transferred to new tubes and stored at −20 °C until MS analysis.

Liquid chromatography-MS (LC-MS) analysis

LC-MS analysis was performed on an LTQ Orbitrap Discovery mass spectrometer (ThermoFisher) coupled to an Agilent 1200 series HPLC. Digests were pressure-loaded onto a 250-μm fused silica desalting column packed with 4 cm of Aqua C18 reverse phase resin (Phenomenex). Digests of affinity-purified samples were loaded in their entirety, whereas unfractionated sample digests were centrifuged (16,873 × g, 4 °C, 2 min) before loading half of each sample onto the column. The peptides were eluted onto a biphasic column (100-μm fused silica with a 5 μm tip, packed with 10 cm C18 and 3 cm Partisphere strong cation exchange resin (SCX, Whatman)). The peptides were eluted from the SCX onto the C18 resin and into the mass spectrometer as previously described[20].

MS data analysis

Tandem-MS data were searched using the SEQUEST algorithm against a combined rabbit and *V. cholerae* (or human and *V. cholerae*) UniProt database using the *V. cholerae* serotype O1 (strain ATCC 39315/El Tor Inaba N16961) proteome (UniProt proteome ID UP000000584). A static modification of +57 on Cys was specified to account for iodoacetamide alkylation. The SEQUEST output files generated from the digests were filtered using DTASelect (v2.0.39). MS data files have been deposited to the ProteomeXchange Consortium[52] via the PRIDE partner repository with the dataset identifier PXD003000. MS data are presented in the form of spectral counts, which is standard for ABPP-MudPIT analyses with FP-biotin[53]. Proteins identified by DTASelect were manually filtered for proteins with ≥2 spectral counts.

Given the intrinsic biological variability of rabbit and human isolates, stringent filtering criteria were applied to identify proteins of interest from MS analyses. Only proteins with a spectral count ratio (FP-biotin/DMSO) ≥5 or no DMSO-associated spectral counts were considered enriched by FP-biotin in ABPP-MudPIT analyses of cecal fluid and human cholera stool supernatants (Supplementary Tables 4–6; Supplementary Data Sets 1A and 2A). To identify serine hydrolases that were significantly more active in cecal fluid from wild-type versus S361A *V. cholerae*-infected rabbits (or vice versa), the following criteria were applied: 1) the protein must be annotated as a serine hydrolase and/or contain a predicted serine hydrolase domain; 2) the MS data must include at least one peptide that is unique to the protein of interest (please see the raw MS data files in the PRIDE repository for a list of unique peptides); 3) the overall fold change in spectral counts between wild-type and S361A samples must be >5 with $P \leq 0.05$ and a false discovery rate ≤0.05 (see "Statistical Analyses" for a description of statistical methods). For comparative proteomic analyses of Δquad versus wild-type cecal fluid, proteins with an overall fold change in spectral counts >5, a lower confidence limit >1, and at least one unique peptide were considered significant.

In-gel trypsin digestion and MS analysis

Cell-free supernatants from wild-type *V. cholerae* biofilm cultures (100 μL, 1.3 mg/mL) were reacted with 5 μM FP-biotin or DMSO for 1 h at rt. Samples were adjusted to 1.1 mL with SDS/PBS (1% (w/v) final SDS concentration), heated for 5 min at 80 °C, and then diluted with PBS to a final SDS concentration of 0.2%. Samples were incubated with 100 μL streptavidin-agarose beads (Thermo Scientific) at 4 °C for 16 h, and then at rt for 3 h. The beads were washed with 0.2% SDS/PBS (5 mL), PBS (3 × 5 mL), and water (3 × 5 mL), then twice with 6 M urea in PBS (600 μL). The beads were pelleted by centrifugation (1400 × g, 4 °C, 3 min) between washes and heated at 95 °C for 5 min in 100 μL 2X SDS-PAGE loading buffer to remove bound proteins. Proteins were separated by SDS-PAGE (4–12% NuPAGE Bis/Tris precast gel) and visualized by silver staining. Proteins detected only in the FP-biotin-labeled sample were excised and submitted to the Taplin Mass Spectrometry Facility of Harvard Medical School (Boston, MA, USA) for in-gel trypsin digestion and MS analysis.

Bioinformatic analyses

Protein sequences of human intelectin-1, intelectin-2, and putative rabbit intelectins (UniProt accession numbers G1U048, G1T5Q3 and G1SS53) were aligned using Clustal Omega[54]. The percent amino acid identity between human intelectin-1 and G1U048 was calculated using the Basic Local Alignment Search Tool (BLAST)[55]. Predicted functional and protein domain annotations of uncharacterized proteins were determined using BLAST and the Simple Modular Architecture Research Tool (SMART)[24]. Rabbit homologues of human serine hydrolases were identified using BLAST (E value $\leq 10^{-80}$ for all homologues).

Fatty acid analyses

Cecal fluid for fatty acid analyses was stored on ice immediately following extraction. The fluid was centrifuged (20,817 × g, 4 °C, 5 min) and the resulting supernatant was syringe-filtered through a 0.45-μm, 13-mm PVDF filter (EMD Millipore). Cell-free supernatants

were stored at −80 °C until analysis. Samples were submitted to the LIPID MAPS Lipidomics Core at the University of California, San Diego (San Diego, California, USA) for extraction and quantification of total and free fatty acids by gas chromatography-MS. A total of 10 cecal fluid isolates (5 each from rabbits infected with either wild-type or Δquad *V. cholerae*) from two separate litters were analyzed to control for litter-specific effects.

Intelectin binding assays

Bacteria grown to mid-exponential phase were centrifuged (5000 × g, rt, 3 min) and resuspended in 20 μL HEPES-buffered saline (140 mM NaCl, 1.5 mM Na_2HPO_4, 50 mM HEPES, pH 7.5) supplemented with 2 mM $CaCl_2$ (HSC) (intelectin binding and elution buffers were formulated as previously described[43]). Cells were incubated with 0.25 μg purified human intelectin-1 (2.5 μL of a 0.1 mg/mL solution; Abcam, ab109151, or Sigma, SRP8047) for 1 h at rt and washed once with an equal volume of HSC. Bound intelectin-1 was eluted in 22.5 μL Tris-buffered saline (150 mM NaCl, 50 mM Tris-Cl, pH 7.5) supplemented with 10 mM EDTA (TSE). Unbound input, wash, and elution fractions were treated with 4X NuPAGE LDS sample buffer (Life Technologies) without reducing agent and incubated at 95 °C for 5 min prior to SDS-PAGE and Western blot analysis. All intelectin binding assays were repeated at least twice with consistent results.

Intelectin elution assays

Cecal fluid for the analysis of endogenous intelectin was stored at rt immediately following extraction. Cells were centrifuged (20,817 × g, 4 °C, 5 min) and washed once with 50 μL HSC or HEPES-buffered saline sans $CaCl_2$ (20,817 × g, 4 °C, 30 sec), then incubated with 50 μL TSE (10 min, rt) to elute bound intelectin. Wash and elution fractions were treated with 4X NuPAGE LDS sample buffer with or without reducing agent (4 mM dithiothreitol) and incubated at 95 °C for 5 min prior to SDS-PAGE and Western blot analysis.

For comparative analyses of endogenous intelectin binding to wild-type or Δquad *V. cholerae*, freshly isolated cecal fluid from infected animals of the same litter and with similar bacterial loads was used to minimize biological variability. Background-subtracted integrated density measurements were calculated using a FLA-5100 imaging system and Multi Gauge V.3.1 software (Fujifilm) and were normalized to the number of CFUs in each sample. These experiments were performed three times with consistent results using cecal fluid isolates from two separate litters to control for litter-specific effects.

Intelectin cleavage assays

Purified human intelectin-1 (0.1 μg) was incubated with 1 μL cell-free cecal fluid (0.45 mg/mL) or PBS for 5 min at rt in 8 μL PBS. Reactions were quenched by adding 4X NuPAGE LDS sample buffer without reducing agent and incubated at 95 °C for 5 min prior to SDS-PAGE and Western blot analysis. These experiments were performed three times with consistent results using three separate cecal fluid isolates from wild-type and Δquad-infected animals.

Statistical Analyses

The majority of data were not normally distributed, and therefore either non-parametric tests or linear models[56, 57] were used for statistical analyses, except where indicated. Standard statistical analyses were performed using GraphPad Prism 6 and Microsoft Excel for Mac 2011 (Version 14.5.2). For ABPP-MudPIT data, a generalized Poisson model (negative binomial) was used to estimate fold changes and approximate 95% confidence intervals. Adjusted *P*-values (i.e., false discovery rates) were calculated using the Benjamini and Hochberg algorithm[58]. For proteomic data, to account for technical replication, a random effects Poisson model was employed to estimate fold changes and confidence limits. Computations used version 3.2 of the R statistical computing environment (www.r-project.org), with specific modeling functions glm.nb and glmmPQL from version 7.3-44 of the MASS library[59]. For certain proteins in the ABPP-MudPIT or proteomic datasets, spectral counts were too sparse to permit convergence of the negative binomial or random effects models; in these cases, the more restricted simple Poisson model was employed for approximate fold change and confidence interval estimation.

Supplementary Material

Refer to Web version on PubMed Central for supplementary material.

Acknowledgments

We gratefully acknowledge Regina LaRocque, Yves Millet, and Jean Lee for reagents and technical assistance and members of the Waldor lab for helpful discussions. We also thank Vincent Carey for the statistical analysis of our MS data and Daniel Bak for help formatting our MS datasets. This work was supported by the National Institutes of Health (R37 AI-042347 to M.K.W.; F31 AI-120665 to T.H.; R01 AI-106878 and U01 AI-058935 to E.T.R.; funding from Institutional Training Grant T32 DK 7477-30 to S.K.H.), the Howard Hughes Medical Institute (M.K.W), the Charles A. King Trust Postdoctoral Fellowship Program, Bank of America, N.A., Co-Trustee (S.K.H.), the Damon Runyon Cancer Research Foundation (DRR-18-12 to E.W.), the Smith Family Foundation (E.W.), and the Swiss National Science Foundation (P300P3_155287/1 to S.A.).

References

1. Ivarsson ME, Leroux JC, Castagner B. Targeting bacterial toxins. Angew Chem Int Ed Engl. 2012; 51:4024–4045. [PubMed: 22441768]
2. Kilian M, Mestecky J, Russell MW. Defense mechanisms involving Fc-dependent functions of immunoglobulin A and their subversion by bacterial immunoglobulin A proteases. Microbiol Rev. 1988; 52:296–303. [PubMed: 3045518]
3. Ruiz-Perez F, Nataro JP. Bacterial serine proteases secreted by the autotransporter pathway: classification, specificity, and role in virulence. Cell Mol Life Sci. 2014; 71:745–770. [PubMed: 23689588]
4. Cravatt BF, Wright AT, Kozarich JW. Activity-based protein profiling: from enzyme chemistry to proteomic chemistry. Annu Rev Biochem. 2008; 77:383–414. [PubMed: 18366325]
5. Puri AW, Bogyo M. Applications of small molecule probes in dissecting mechanisms of bacterial virulence and host responses. Biochemistry. 2013; 52:5985–5996. [PubMed: 23937332]
6. Ritchie JM, Waldor MK. *Vibrio cholerae* interactions with the gastrointestinal tract: lessons from animal studies. Curr Top Microbiol Immunol. 2009; 337:37–59. [PubMed: 19812979]
7. Sikora AE. Proteins secreted via the type II secretion system: smart strategies of *Vibrio cholerae* to maintain fitness in different ecological niches. PLoS Pathog. 2013; 9:e1003126. [PubMed: 23436993]

8. Simon GM, Cravatt BF. Activity-based proteomics of enzyme superfamilies: serine hydrolases as a case study. J Biol Chem. 2010; 285:11051–11055. [PubMed: 20147750]
9. Kidd D, Liu Y, Cravatt BF. Profiling serine hydrolase activities in complex proteomes. Biochemistry. 2001; 40:4005–4015. [PubMed: 11300781]
10. Patricelli MP, Giang DK, Stamp LM, Burbaum JJ. Direct visualization of serine hydrolase activities in complex proteomes using fluorescent active site-directed probes. Proteomics. 2001; 1:1067–1071. [PubMed: 11990500]
11. Shaw DK, Hyde JA, Skare JT. The BB0646 protein demonstrates lipase and haemolytic activity associated with *Borrelia burgdorferi*, the aetiological agent of Lyme disease. Mol Microbiol. 2012; 83:319–334. [PubMed: 22151008]
12. Weadge JT, Clarke AJ. *Neisseria gonorrheae* O-acetylpeptidoglycan esterase, a serine esterase with a Ser-His-Asp catalytic triad. Biochemistry. 2007; 46:4932–4941. [PubMed: 17388571]
13. Stroud RM, Kossiakoff AA, Chambers JL. Mechanisms of zymogen activation. Annu Rev Biophys Bioeng. 1977; 6:177–193. [PubMed: 17350]
14. Gloeckl S, et al. Identification of a serine protease inhibitor which causes inclusion vacuole reduction and is lethal to *Chlamydia trachomatis*. Mol Microbiol. 2013; 89:676–689. [PubMed: 23796320]
15. Hauske P, et al. Selectivity profiling of DegP substrates and inhibitors. Bioorg Med Chem. 2009; 17:2920–2924. [PubMed: 19233659]
16. Steuber H, Hilgenfeld R. Recent advances in targeting viral proteases for the discovery of novel antivirals. Curr Top Med Chem. 2010; 10:323–345. [PubMed: 20166951]
17. Tsuji S, et al. Human intelectin is a novel soluble lectin that recognizes galactofuranose in carbohydrate chains of bacterial cell wall. J Biol Chem. 2001; 276:23456–23463. [PubMed: 11313366]
18. Ritchie JM, Rui H, Bronson RT, Waldor MK. Back to the future: studying cholera pathogenesis using infant rabbits. MBio. 2010; 1:e00047–10. [PubMed: 20689747]
19. Bachovchin DA, et al. A high-throughput, multiplexed assay for superfamily-wide profiling of enzyme activity. Nat Chem Biol. 2014; 10:656–663. [PubMed: 24997602]
20. Weerapana E, Speers AE, Cravatt BF. Tandem orthogonal proteolysis-activity-based protein profiling (TOP-ABPP)--a general method for mapping sites of probe modification in proteomes. Nat Protoc. 2007; 2:1414–1425. [PubMed: 17545978]
21. The UniProt Consortium. UniProt: a hub for protein information. Nucleic Acids Res. 2015; 43:D204–212. [PubMed: 25348405]
22. Faruque SM, et al. Transmissibility of cholera: in vivo-formed biofilms and their relationship to infectivity and persistence in the environment. Proc Natl Acad Sci USA. 2006; 103:6350–6355. [PubMed: 16601099]
23. Tamayo R, Patimalla B, Camilli A. Growth in a biofilm induces a hyperinfectious phenotype in *Vibrio cholerae*. Infect Immun. 2010; 78:3560–3569. [PubMed: 20515927]
24. Schultz J, Milpetz F, Bork P, Ponting CP. SMART, a simple modular architecture research tool: identification of signaling domains. Proc Natl Acad Sci USA. 1998; 95:5857–5864. [PubMed: 9600884]
25. Yeats C, Bentley S, Bateman A. New knowledge from old: in silico discovery of novel protein domains in Streptomyces coelicolor. BMC Microbiol. 2003; 3:3. [PubMed: 12625841]
26. Gadwal S, Korotkov KV, Delarosa JR, Hol WG, Sandkvist M. Functional and structural characterization of *Vibrio cholerae* extracellular serine protease B, VesB. J Biol Chem. 2014; 289:8288–8298. [PubMed: 24459146]
27. Sikora AE, Zielke RA, Lawrence DA, Andrews PC, Sandkvist M. Proteomic analysis of the *Vibrio cholerae* type II secretome reveals new proteins, including three related serine proteases. J Biol Chem. 2011; 286:16555–16566. [PubMed: 21385872]
28. Siezen RJ, Leunissen JA. Subtilases: the superfamily of subtilisin-like serine proteases. Protein Sci. 1997; 6:501–523. [PubMed: 9070434]
29. Altindis E, Fu Y, Mekalanos JJ. Proteomic analysis of *Vibrio cholerae* outer membrane vesicles. Proc Natl Acad Sci USA. 2014; 111:E1548–1556. [PubMed: 24706774]

30. Smith DR, et al. In situ proteolysis of the *Vibrio cholerae* matrix protein RbmA promotes biofilm recruitment. Proc Natl Acad Sci USA. 2015; 112:10491–10496. [PubMed: 26240338]
31. Park BR, et al. A metalloprotease secreted by the type II secretion system links *Vibrio cholerae* with collagen. J Bacteriol. 2015; 197:1051–1064. [PubMed: 25561716]
32. Chalfoun NR, et al. Purification and characterization of AsES protein: a subtilisin secreted by *Acremonium strictum* is a novel plant defense elicitor. J Biol Chem. 2013; 288:14098–14113. [PubMed: 23530047]
33. Mandlik A, et al. RNA-Seq-based monitoring of infection-linked changes in *Vibrio cholerae* gene expression. Cell Host Microbe. 2011; 10:165–174. [PubMed: 21843873]
34. Fiore AE, Michalski JM, Russell RG, Sears CL, Kaper JB. Cloning, characterization, and chromosomal mapping of a phospholipase (lecithinase) produced by *Vibrio cholerae*. Infect Immun. 1997; 65:3112–3117. [PubMed: 9234762]
35. Pride AC, Herrera CM, Guan Z, Giles DK, Trent MS. The outer surface lipoprotein VolA mediates utilization of exogenous lipids by Vibrio cholerae. MBio. 2013; 4:e00305–13. [PubMed: 23674613]
36. Lundwall A, Brattsand M. Kallikrein-related peptidases. Cell Mol Life Sci. 2008; 65:2019–2038. [PubMed: 18344018]
37. Holmes RS, Cox LA. Comparative Structures and Evolution of Vertebrate Carboxyl Ester Lipase (CEL) Genes and Proteins with a Major Role in Reverse Cholesterol Transport. Cholesterol. 2011; 2011:781643. [PubMed: 22162806]
38. Pedersen LL, Turco SJ. Galactofuranose metabolism: a potential target for antimicrobial chemotherapy. Cell Mol Life Sci. 2003; 60:259–266. [PubMed: 12678491]
39. Wrackmeyer U, Hansen GH, Seya T, Danielsen EM. Intelectin: a novel lipid raft-associated protein in the enterocyte brush border. Biochemistry. 2006; 45:9188–9197. [PubMed: 16866365]
40. Pemberton AD, et al. Innate BALB/c enteric epithelial responses to Trichinella spiralis: inducible expression of a novel goblet cell lectin, intelectin-2, and its natural deletion in C57BL/10 mice. J Immunol. 2004; 173:1894–1901. [PubMed: 15265922]
41. Voehringer D, et al. *Nippostrongylus brasiliensis*: identification of intelectin-1 and -2 as Stat6-dependent genes expressed in lung and intestine during infection. Exp Parasitol. 2007; 116:458–466. [PubMed: 17420014]
42. Ellis CN, et al. Comparative proteomic analysis reveals activation of mucosal innate immune signaling pathways during cholera. Infect Immun. 2015; 83:1089–1103. [PubMed: 25561705]
43. Tsuji S, et al. Capture of heat-killed Mycobacterium bovis bacillus Calmette-Guerin by intelectin-1 deposited on cell surfaces. Glycobiology. 2009; 19:518–526. [PubMed: 19179460]
44. Varina M, Denkin SM, Staroscik AM, Nelson DR. Identification and characterization of Epp, the secreted processing protease for the *Vibrio anguillarum* EmpA metalloprotease. J Bacteriol. 2008; 190:6589–6597. [PubMed: 18689477]
45. Bracco U. Effect of triglyceride structure on fat absorption. Am J Clin Nutr. 1994; 60:1002S–1009S. [PubMed: 7977140]
46. Drzazga A, Sowinska A, Koziolkiewicz M. Lysophosphatidylcholine and lysophosphatidylinosiol--novel promissing signaling molecules and their possible therapeutic activity. Acta Pol Pharm. 2014; 71:887–899. [PubMed: 25745761]
47. Wesener DA, et al. Recognition of microbial glycans by human intelectin-1. Nat Struct Mol Biol. 2015; 22:603–610. [PubMed: 26148048]
48. Suzuki YA, Shin K, Lonnerdal B. Molecular cloning and functional expression of a human intestinal lactoferrin receptor. Biochemistry. 2001; 40:15771–15779. [PubMed: 11747454]
49. Yang RZ, et al. Identification of omentin as a novel depot-specific adipokine in human adipose tissue: possible role in modulating insulin action. Am J Physiol Endocrinol Metab. 2006; 290:E1253–1261. [PubMed: 16531507]
50. Hatzios SK, Ringgaard S, Davis BM, Waldor MK. Studies of dynamic protein-protein interactions in bacteria using Renilla luciferase complementation are undermined by nonspecific enzyme inhibition. PLoS One. 2012; 7:e43175. [PubMed: 22905225]
51. Abel S, Waldor MK. Infant rabbit model for diarrheal diseases. Curr Protoc Microbiol. 2015; 38:6A.6.1–6A.6.15. [PubMed: 26237109]

52. Vizcaino JA, et al. ProteomeXchange provides globally coordinated proteomics data submission and dissemination. Nat Biotechnol. 2014; 32:223–226. [PubMed: 24727771]

53. Kamat SS, et al. Immunomodulatory lysophosphatidylserines are regulated by ABHD16A and ABHD12 interplay. Nat Chem Biol. 2015; 11:164–171. [PubMed: 25580854]

54. Sievers F, et al. Fast, scalable generation of high-quality protein multiple sequence alignments using Clustal Omega. Mol Syst Biol. 2011; 7:539. [PubMed: 21988835]

55. Altschul SF, Gish W, Miller W, Myers EW, Lipman DJ. Basic local alignment search tool. J Mol Biol. 1990; 215:403–410. [PubMed: 2231712]

56. Breslow NE, Clayton DG. Approximate interference in generalized linear mixed models. J Am Stat Assoc. 1993; 88:9–25.

57. Wolfinger R, O'Connell M. Generalized linear mixed models: a pseudo-likelihood approach. J Stat Comput Simul. 1993; 48:233–243.

58. Benjamini Y, Hochberg Y. Controlling the false discovery rate: a practical and powerful approach to multiple testing. J R Statist Soc B. 1995; 57:289–300.

59. Venables, WN.; Ripley, BD. Modern Applied Statistics with S. Fourth Edition. Springer; 2002.

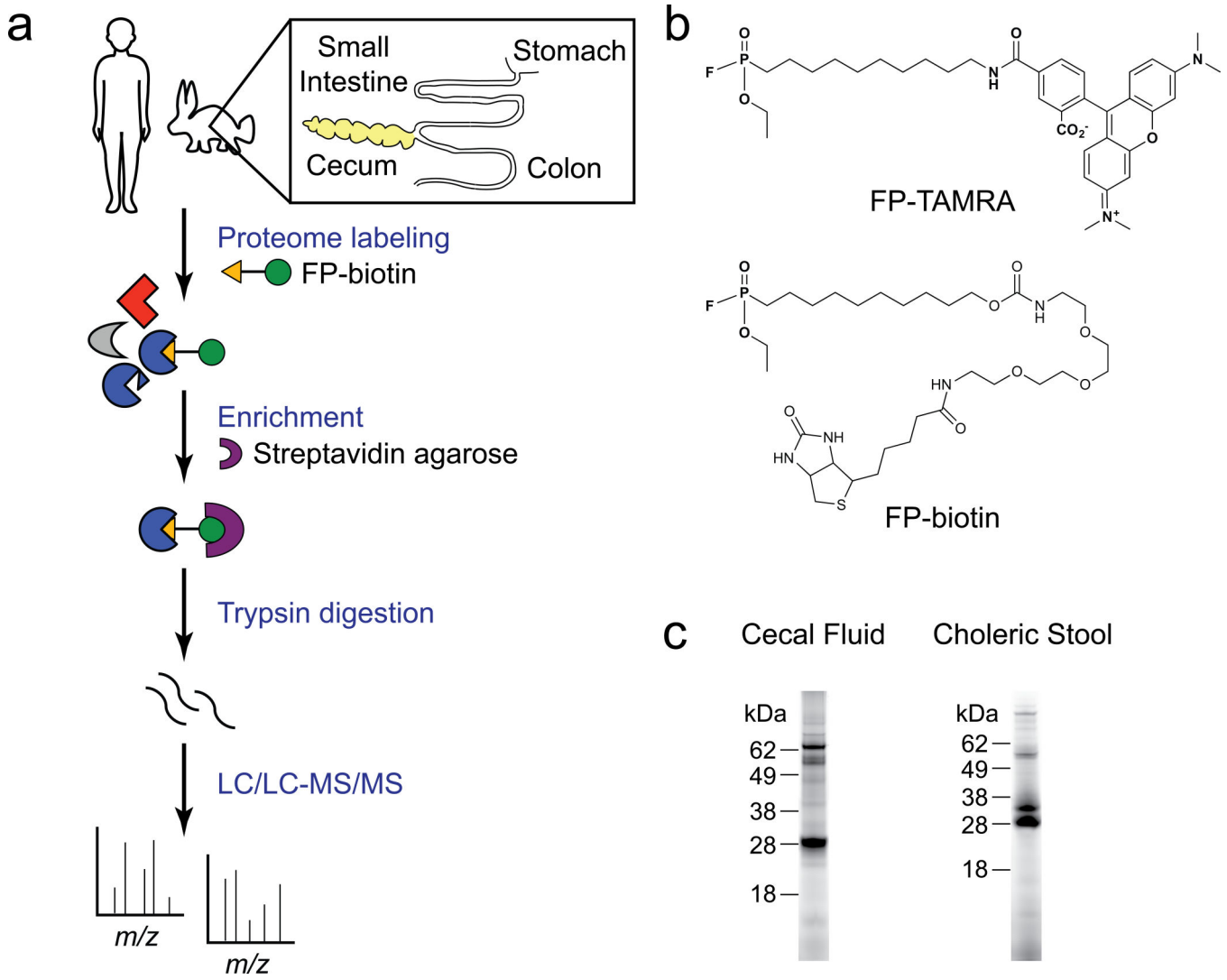

Figure 1. ABPP detects active serine hydrolases in rabbit cecal fluid and human cholera stool

(**a**) Active serine hydrolases in human cholera stool and rabbit cecal fluid supernatants were selectively labeled with FP-biotin, enriched with streptavidin agarose, and digested with trypsin prior to MS analysis. (**b**) Chemical structures of the FP-TAMRA and FP-biotin ABPs. (**c**) ABPP gels of FP-TAMRA-labeled supernatants from rabbit cecal fluid and human cholera stool.

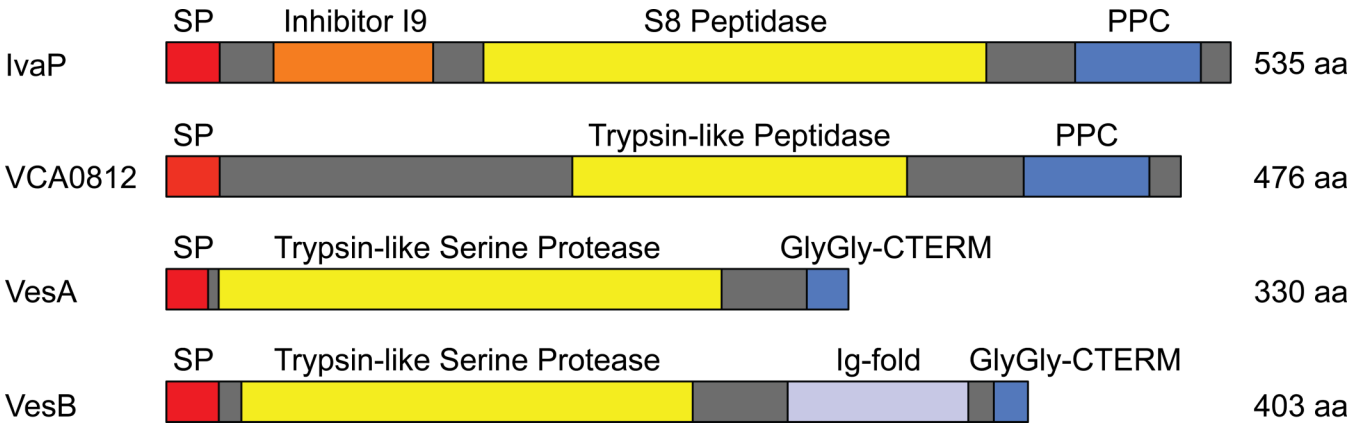

Figure 2. Predicted protein domain structures of IvaP, VCA0812, VesA, and VesB

All four *V. cholerae* serine hydrolases that were consistently detected in FP-biotin-enriched cecal fluid isolates contain conserved N-terminal signal peptide (SP; red), serine protease (yellow), and C-terminal domains (bacterial pre-peptidase PPC or GlyGly-CTERM; blue). In addition, IvaP contains an N-terminal peptidase inhibitor I9 domain (orange), and VesB contains a C-terminal Ig-fold domain (light purple).

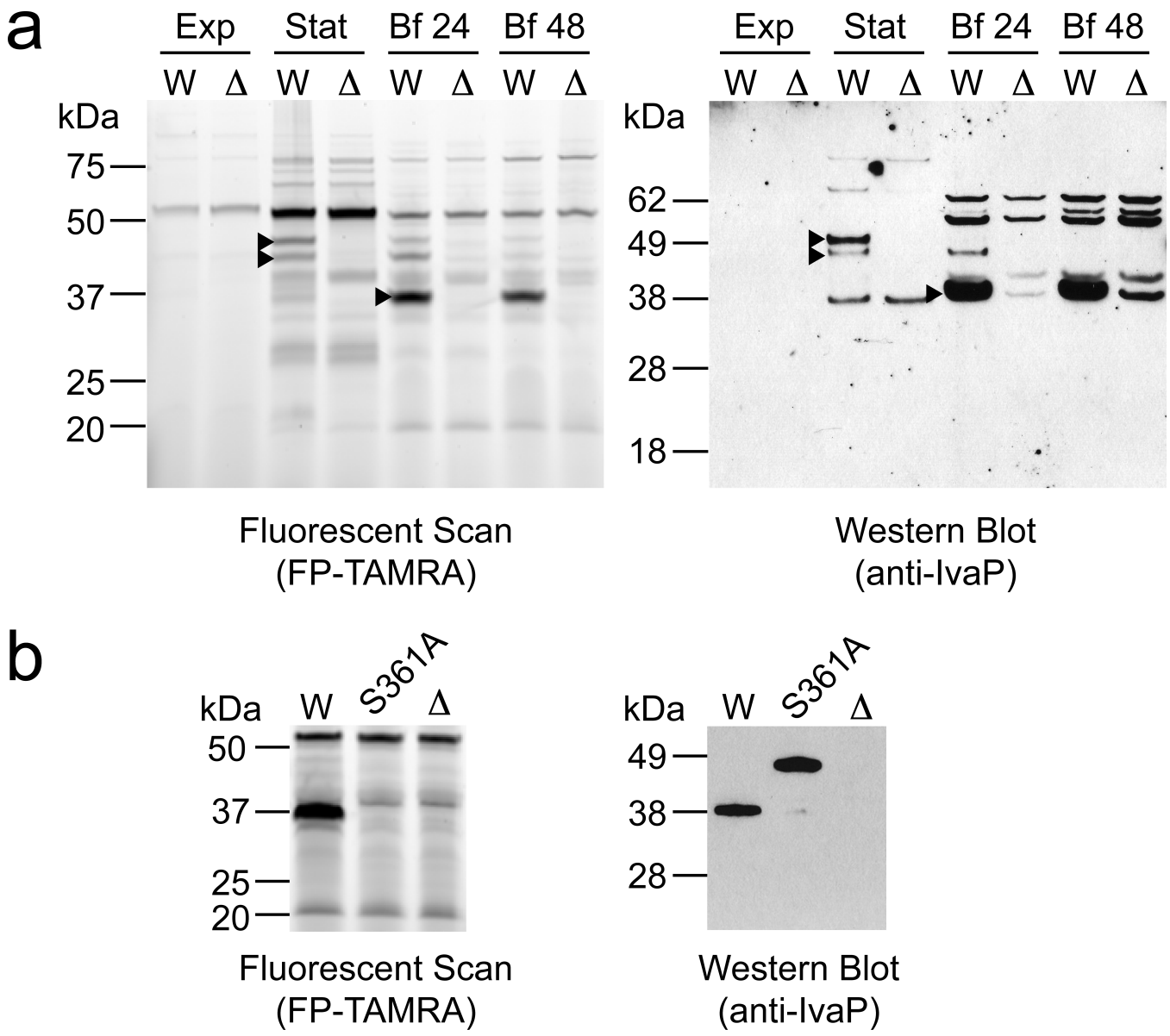

Figure 3. IvaP undergoes growth phase-dependent processing and autoproteolysis

(**a**) ABPP gel (left) and Western blot (right, using polyclonal anti-IvaP antisera) of FP-TAMRA-labeled supernatants from exponential phase (Exp), stationary phase (Stat), and biofilm cultures grown for 24 h (Bf 24) or 48 h (Bf 48). Supernatants (each containing 0.25 mg/mL total protein) were derived from both wild-type (W) and Δ*ivaP* (Δ) *V. cholerae* cultures. Black arrowheads denote the molecular weights of IvaP-specific protein bands. (**b**) ABPP gel (left) and Western blot (right) of FP-TAMRA-labeled supernatants from wild-type (W), Δ*ivaP::ivaP*^{Ser361Ala} (S361A), and Δ*ivaP* (Δ) *V. cholerae* biofilm cultures grown for 48 h.

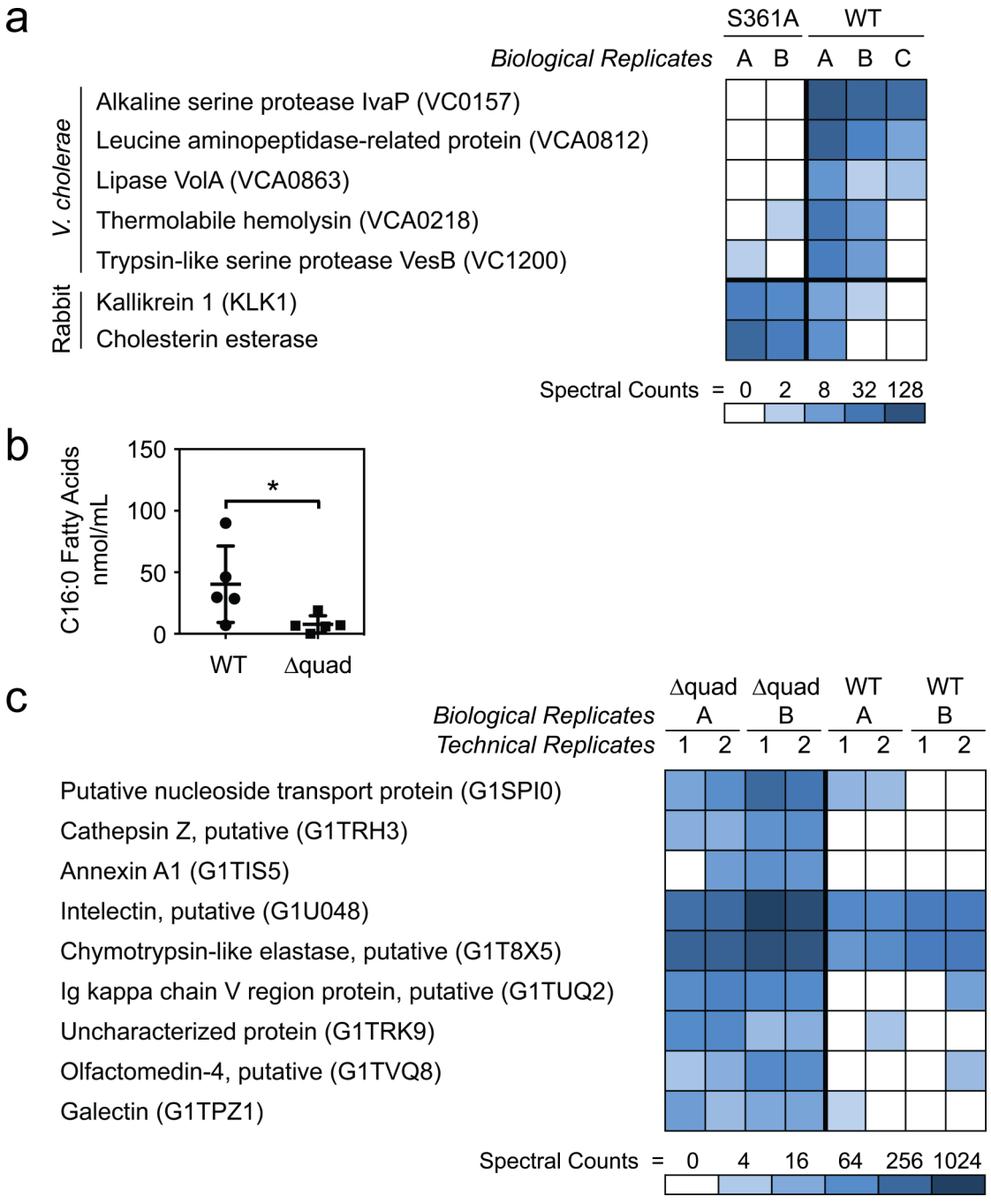

Figure 4. *V. cholerae* proteases alter the serine hydrolase activity, lipid profile, and protein content of rabbit cecal fluid

(**a**) Heat map depicting the number of spectral counts detected in FP-biotin-enriched cecal fluid supernatants from rabbits infected with wild-type (WT) or S361A *V. cholerae*. Serine hydrolases with a >5-fold change in spectral counts between WT and S361A isolates (or vice versa), an associated $P \leq 0.05$, and at least one unique peptide are shown. Only IvaP, VCA0812, and KLK1 had an adjusted $P \leq 0.05$ following a correction for multiple testing. Data are from 2 or 3 biological replicates (A-C). See Supplementary Tables 7 and 8 and

Supplementary Data Set 1B for a complete list and associated statistics. (**b**) Concentrations of total (esterified and non-esterified) C16:0 fatty acids detected in the cecal fluid of rabbits infected with WT or Δquad *V. cholerae*. Each data point represents a single rabbit. Horizontal bars represent mean ± s.d. for 5 biological replicates. **P* <0.02 by the Mann-Whitney test. (**c**) Heat map depicting the number of spectral counts detected in the cecal contents of rabbits infected with WT or Δquad *V. cholerae*. Proteins with a >5-fold change in spectral counts in Δquad versus WT isolates, a lower confidence limit >1, and at least one unique peptide are shown. Data are from 2 biological replicates (A and B) with 2 corresponding technical replicates (1 and 2). UniProt accession numbers are shown in parentheses. See Supplementary Table 9 and Supplementary Data Set 6B for a complete list and associated statistics.

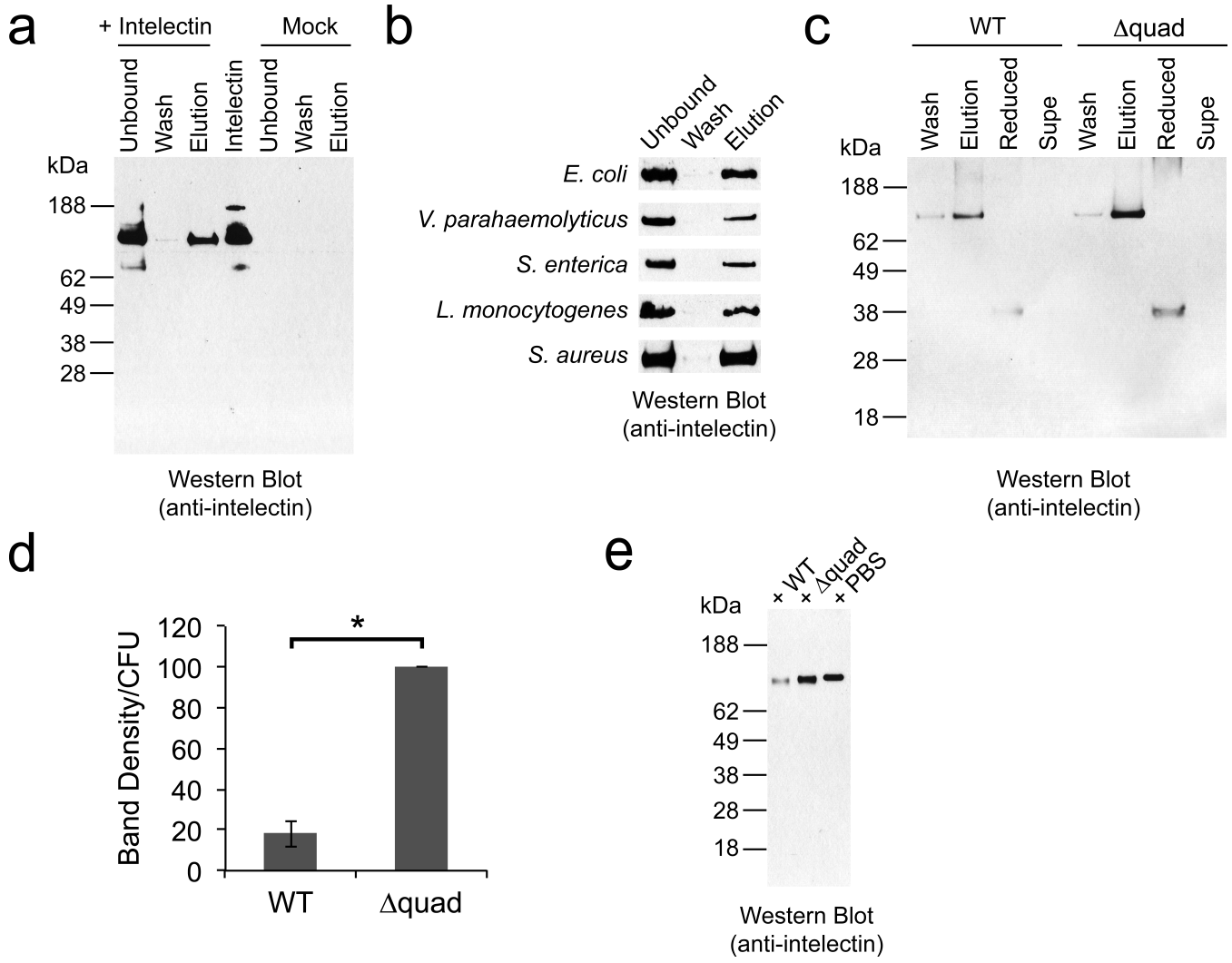

Figure 5. *V. cholerae* proteases decrease intelectin binding to *V. cholerae* in infected rabbits

(**a**) Western blot of recombinant human intelectin-1 incubated with *V. cholerae* cells. Unbound, wash, and EDTA-eluted protein fractions were analyzed under non-reducing conditions alongside purified intelectin and fractions from cells treated with buffer alone (mock) using a polyclonal intelectin-1 antibody. (**b**) Western blots of recombinant human intelectin-1 incubated with *E. coli*, *V. parahaemolyticus*, *S. enterica*, *L. monocytogenes*, and *S. aureus* cells. Protein fractions were analyzed under non-reducing conditions. See Supplementary Fig. 9 for full-length blots. (**c**) Western blot of endogenous intelectin bound to wild-type (WT) and Δquad *V. cholerae* cells in rabbit cecal fluid. Cells were washed once with calcium-containing buffer and then EDTA. Wash, EDTA-treated, and cecal fluid supernatant (Supe) fractions were analyzed under non-reducing conditions. EDTA-eluted proteins were also analyzed in the presence of reducing agent (Reduced). (**d**) Densitometry analysis of EDTA-eluted intelectin from WT and Δquad *V. cholerae* cells in rabbit cecal fluid. Band densities were normalized by CFUs as described in the Online Methods and then expressed as a percentage of the value calculated for Δquad *V. cholerae* in each sample pair. Data represent the average of three biological replicates ± s.d. **P* <0.0025 by the paired

Student's *t*-test (two-tailed). (**e**) Western blot of recombinant human intelectin-1 incubated with PBS or cecal fluid supernatants from rabbits infected with WT or Δquad *V. cholerae* for 5 min at rt. Samples were analyzed under non-reducing conditions.